A study of the temperature distribution in the OTEC cold water pipe using a heat and mass transfer approach

A study of the temperature distribution in the OTEC cold water pipe using a heat and mass transfer approach

A I Firmansyah[1,2*], Mukhtasor[1], D Satrio[1*], S Rahmawati[1], H Ikhwani[1], W A Pratikto[1]

[1] Department of Ocean Engineering, Faculty of Marine Technology, Institut Teknologi Sepuluh Nopember, Surabaya 60111, Indonesia
[2] Research Centre for Energy Conversion and Conservation (PRKKE), National Research and Innovation Agency (BRIN), B. J. Habibie Science and Technology Park Building 620, South Tangerang, Indonesia

*E-mail: 7020221004@student.its.ac.id; dendy.satrio@its.ac.id

Abstract. The difference between sea water temperature at a depth of around 1000 m and sea water temperature at sea level is generally used as a parameter in the design of Ocean Thermal Energy Conversion (OTEC). In practice, electricity generation is determined by the difference between the temperature of the cold seawater coming out of the Cold Water Pipe (CWP) and the temperature of the seawater at the surface. The temperature of cold sea water increases due to heat transfer experienced by cold sea water flowing through the CWP, which comes into contact with surrounding sea water which has a higher temperature. This in turn provides a lower actual temperature difference, and therefore reduces the design power capacity. However, many previous studies did not consider these lower temperature differences. This may be acceptable for cases with practically small heat transfer such as CWP with low thermal conductivity combined with good insulation used in 1000 m CWP vertical floating systems. Unfortunately, this may not be the case for many of OTEC's proposed alternative sites, which are located on land systems that require CWP lengths of five km or more. This raises the need for careful investigation to determine the temperature of the sea water coming out of the CWP, where it is necessary to calculate the temperature distribution of the cold sea water flowing through the CWP. This paper aims to estimate the temperature distribution of cold sea water flowing through the CWP and the increase in temperature of cold sea water leaving the CWP. Analysis based on the principles of mass and heat transfer was carried out in this research, where modelling was carried out numerically using a finite volume approach. For the case considered, the change in sea water temperature at CWP from depth to the surface occurs 1-3^{O}C, which is the accumulation of each change in sea water depth. The results of this research illustrate that designing an OTEC system with a long CWP must consider the temperature distribution of cold sea water flowing through the CWP to produce a more realistic design.

Keywords: Ocean renewable energy; OTEC; CWP; Heat and mass transfer; Temperature distribution.

1. Introduction

The amount of electricity consumed nationally grows at a rate of up to 6 % annually, which is inversely proportional to Indonesia's availability of fossil fuels as a primary energy source [1]. The utilization of primary energy from renewable energy is necessary to meet the electrical demand in Indonesia, which is in line with Presidential Regulation No. 112/2023 concerning accelerating the development of renewable energy for the electricity supply [2]. Indonesia has many renewable energy potential, including ocean energy, because more than 63% of its territory is sea [3–5]. The ocean current energy [6–9] and wave energy [10–12] have been widely developed in Indonesia. Ocean thermal is one of the ocean energy potentials that has yet to be developed, where the potential is 4247.39 GW and practically is 41 GW [13].

The technology for converting ocean thermal to electricity is OTEC (Ocean Thermal Energy Conversion), which utilizes the temperature difference in the deep sea (3-10◦C) and on the surface (20-30°C) to produce electricity [14]. The difference between the surface and deep temperature of seawater is used to operate a Rankine cycle, which produces the rotation of a turbine that drives a generator to produce electricity. Figure 1 illustrates the Rankine Cycle used in Ocean Thermal Energy Conversion (OTEC). In this cycle, cold water from the deep sea is directed towards the heat exchanger [15,16], specifically the condenser [17], where it facilitates the transition of the working fluid from a two-phase state to a saturated liquid form. On the other hand, warm water originating from surface sea streams is directed towards a heat exchanger, specifically an evaporator. The purpose of this heat exchanger is to facilitate the transformation of a subcooled liquid phase of a working fluid into a state of saturation vapor. This vapor is then used to power a rotating turbine and generator, ultimately generating electricity [18][19].

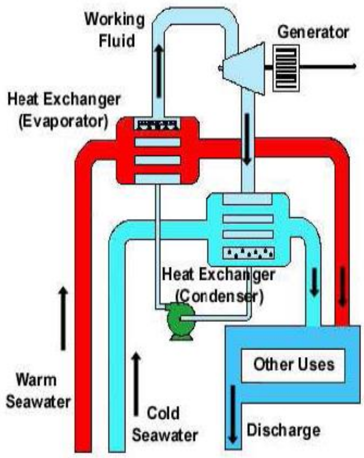

Figure 1. Schematic OTEC [20].

The difference between seawater temperature at typically about 1000 m depth and that at about seawater surface is commonly used as a parameter in the design of the OTEC [21][22]. In practice, the power generation is dictated by the difference between the temperature of the cold seawater coming out of the Cold-Water Pipe (CWP) and that of the surface seawater. The cold seawater temperature increases because of the heat transfer experienced by the cold seawater flowing through the CWP, which is in contact with the ambient seawater at a higher temperature. This in turn gives a lower actual temperature difference, and therefore reduces design power capacity. However, many previous studies did not consider this lower temperature difference. This might be acceptable for the case with a practically small heat transfer such as a CWP with a low heat conductivity combined with a good insulation used in a vertical floating system of 1000 m CWP. Unfortunately, this may not be the case for many alternative sites of proposed OTEC, which are situated at onshore systems requiring a long CWP in the order of five or more km length [23][24]. This rises a need of a careful investigation to define the seawater temperature coming out of the CWP, in which it is necessary to calculate the temperature distribution of the cold seawater flowing through the CWP. This paper aims at estimating the temperature distribution of the cold seawater flowing through the CWP and the increase in the temperature of the cold seawater coming out of the CWP.

2. Data Analysis

2.1. *Ocean Thermal Resources*

In this paper, an analysis of the potential location of marine heat was carried out by Research and Development Center for Marine Geology (MGI) in the northern waters of Bali Island. The site is at latitude 8°5'59" S and longitude 115°22'25"E, with the distance to land 5 km [24]. The research site is shown in figure 2.

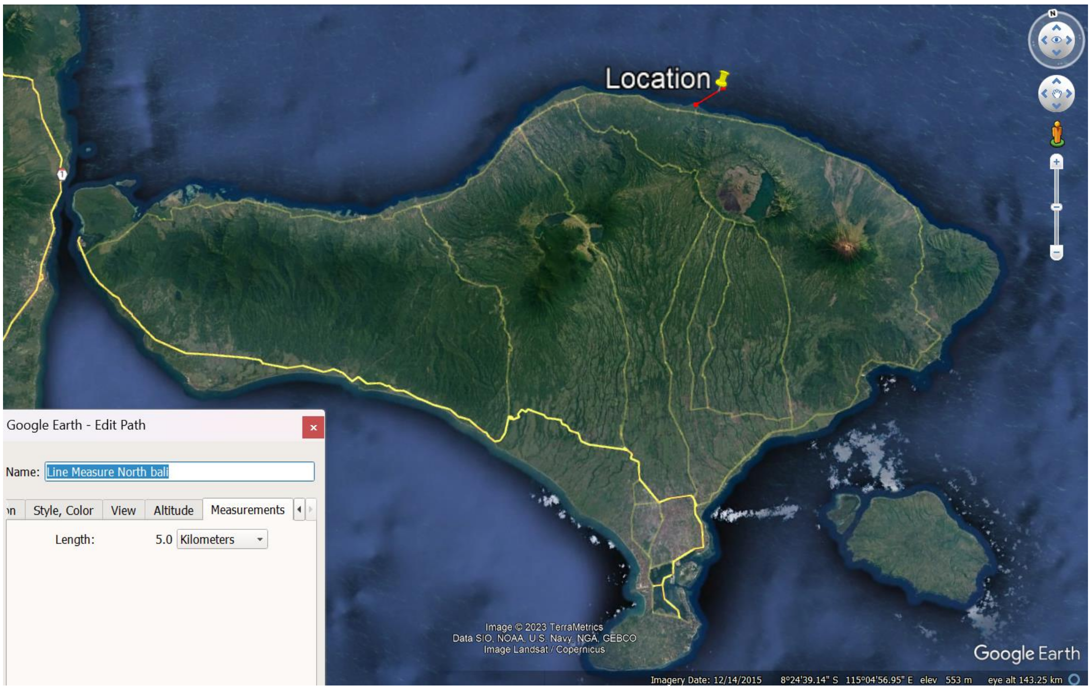

Figure 2. Site of ocean thermal in Northern Bali Island.

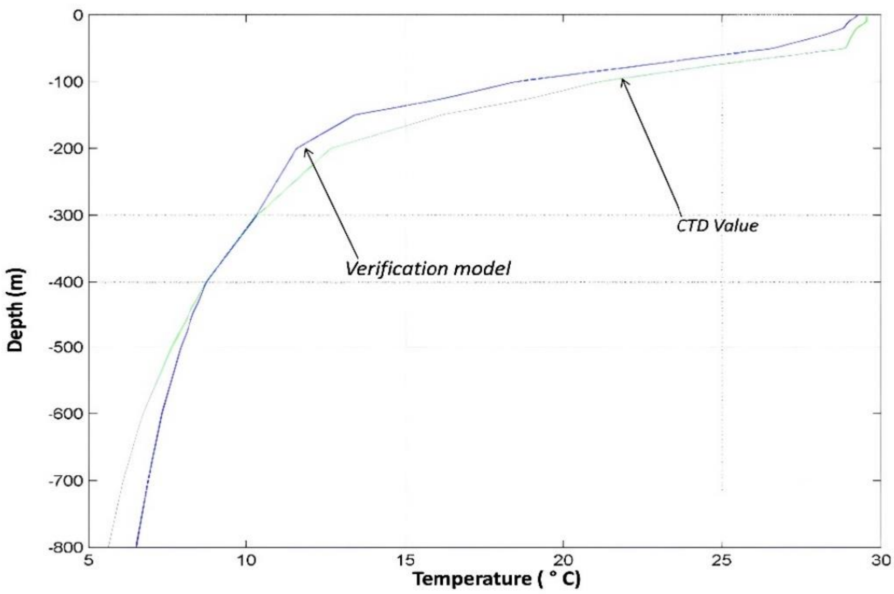

Figure 3. Results of measurement: conductivity, temperature, and depth (CTD) [24].

Figure 3 shows the recorded data concerning the depth and temperature of seawater, as obtained from the CTD instrument. A difference in temperature of 23.3 ºC is calculated between the surface and the deep layers of seawater. The recorded temperature at a seafloor of 800 meters is 5.7 ºC, while the temperature at the surface is 29.1 ºC. In this paper, the assumption is used that changes in CWP depth change per 100 m of seawater depth, followed by changes in seawater temperature. The length of the CWP is divided into eight segments with 625 m each per segment to calculate the heat transfer that occurs in the water mass in the CWP with sea water temperature [25]. For calculating each temperature at each depth, equation (1) was used to approach the depth and temperature in the northern waters of Bali Island, which was carried out by MGI research [23]. The Equation used is as follows:

$$b = (X_n - X_0)/y \quad (1)$$

Where b is a constant function of depth, ($X_n - X_0$) is the difference between seawater temperature surface and depth, and y is depth of sea, the b value is -0.0292. In table 1, estimates of seawater temperature based on depth are shown.

Table 1. Temperature of the seawater based on depth.

Depth (m)	Temperature seawater (ºC)
0	29.1
100	26.2
200	23.2
300	20.3
400	17.4
500	14.5
600	11.6
700	8.6
800	5.7

2.2. *Cold Water Pipe (CWP)*

The CWP material in this research is a standard 12-inch steel pipe used in the oil and gas industry with American Petroleum Institute (API) 5L specifications [26]. Aluminium and High-density Polyethylene (HDPE) were also considered as comparison materials to validate the calculations [25]. API 5L pipe is used to extend the operational life of oil and gas platform equipment which has entered the decommissioning stage but has not yet been carried out due to financial constraints [27–29]. In addition, the application of API 5L pipe is designed to reduce OTEC's Levelized Cost of Energy (LCOE) [30,31], which reaches 13% of OTEC's LCOE. The following are the specifications of the CWP material used in this research:

Tabel 2. Specifications of material [25][32].

No	Parameter	API 5 L	Aluminium	HDPE
1.	Mass Density	7840 kg/m^3	2800 kg/m^3	970 kg/m^3
2.	Thermal Conductivity	42 W/m.K	162 W/m.K	0.43 W/m.K
3.	Specific Heat	430 J/kg.K	871 J/kg.K	2300 J/kg.K
4.	Outside Diameter		323.8 mm	
5.	Thickness		17.48 mm	

3. Method

3.1. *Mass Flow at CWP*

The data collection of the mass flow rate at CWP was conducted based on assumptions aligned with the mass flow rate observed at the 20 kW OTEC pilot plant constructed by the Korea Research Institute of Ships & Ocean Engineering (KRISO). The OTEC system in the pilot plant requires a seawater mass flow rate of 44.85 kg/s in the CWP to feed the purpose of altering the working fluid in the condenser [6]. The flow rate analysis in CWP is further conducted by employing the flow rate diagram specified for schedule 40 as allowed by American Standard Testing and Material (ASTM A53 (www.engineeringtoolbox.com). This diagram considers a seawater discharge velocity of 0.05 m/s and an internal diameter of 0.306 m, applicable to a 12-inch pipe (figure 4).

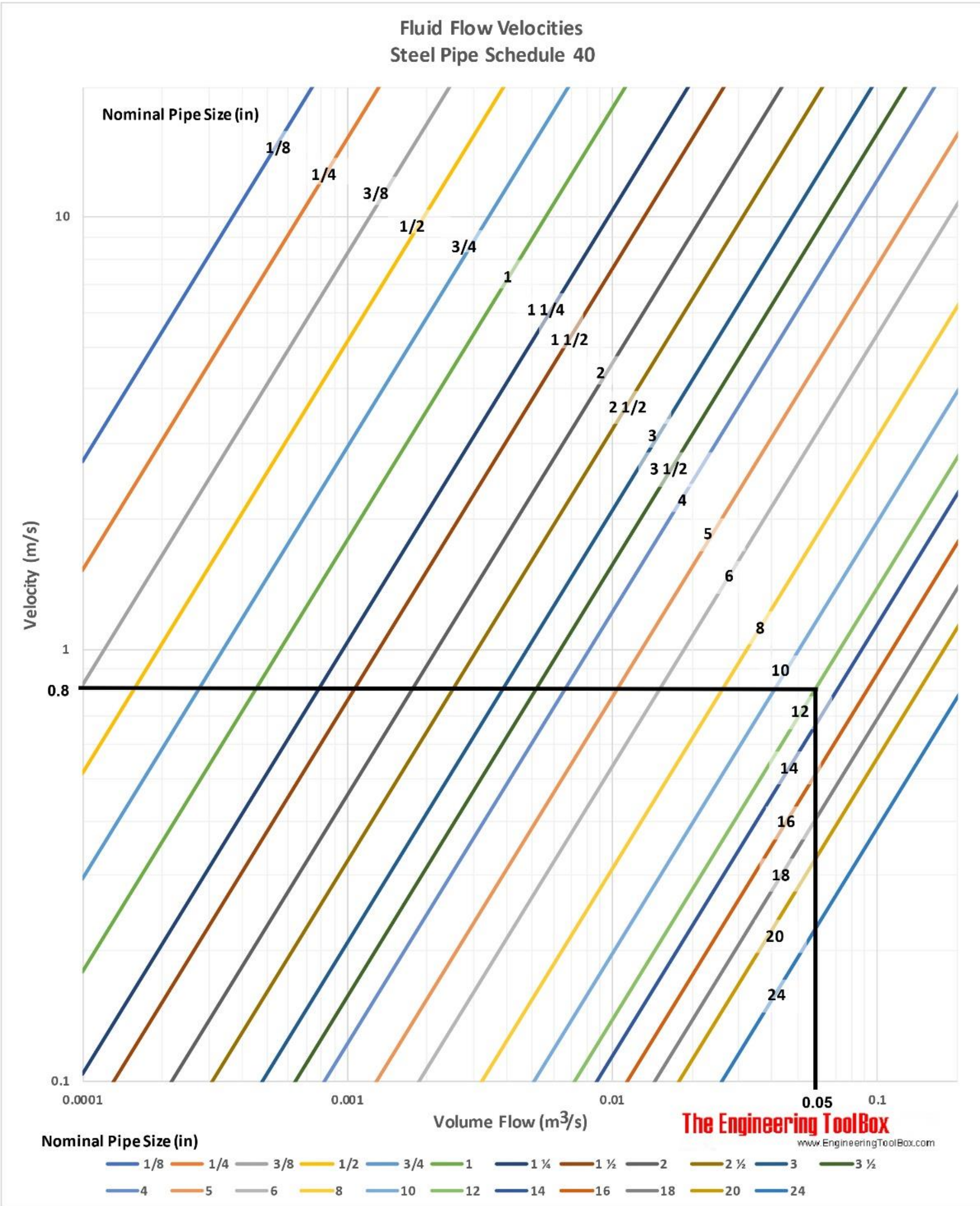

Figure 4. Fluid flow velocities diagram Schedule 40.

3.2. Heat and Mass Transfers Analysis

3.2.1. Mathematical Model.

The purpose of this study was to conduct a heat and mass transfer analysis to gather data on the environmental temperature. This analysis focused on the variations in sea depth on the CWP surface, which in turn influenced the temperature of the mass flow of seawater within the CWP (figure 5). The equations employed in computing heat and mass transfer phenomena are presented as follows [33] :

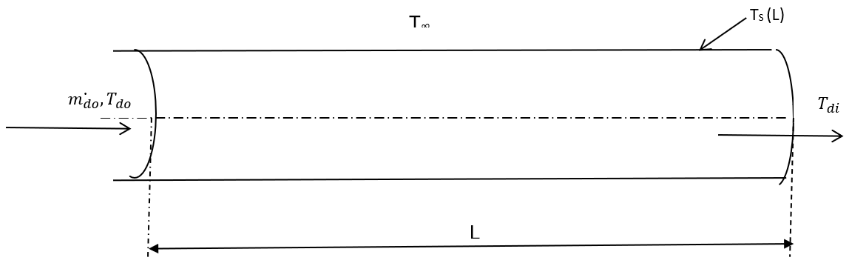

Figure 5. Schematic of heat and mass transfer in CWP.

$$\ddot{q}_s(L) = \frac{T_{di} - T_\infty}{\left[\frac{1}{h_x(L)}\right] + \left[\frac{1}{h_0}\right]} \quad (2)$$

Where $\ddot{q}_s(L)$ is the heat flux along the pipe (w/m2); T_{di} is the temperature of the seawater flow in the pipe along the pipe (°C); T_∞ is sea water temperature (°C); h_x (L) is the inside convection heat transfer at $x=L$ and h_o is the convection heat transfer from seawater to the pipe surface. The equation used in calculating the h_x value is as follows:

$$Re_d = \frac{4\dot{m}_{do}}{\pi D \mu} \quad (3)$$

$$Nu_D = 0.023 Re_D^{4/5} Pr_d^{\ 0.3} \quad (4)$$

$$h_x(L) = Nu_d \frac{k}{D} \quad (5)$$

Where Re_d is the Reynolds number of the fluid inside the pipe; $\dot{m}_{do}$ is the fluid flow in the pipe (kg/s); D is the pipe diameter (m); μ is viscosity dynamics (N.s/m^2); Nu_D is the Nusselt number of the pipe; Pr_d is the Prandtl Number of the pipe and k is the thermal conductivity (W/m.K). The equation used to calculate the T_s (L) value is the temperature at the pipe surface (°C), as follows:

$$\ddot{q}_s(L) = \frac{T_{di} - T_s}{\frac{1}{h_x}(L)} \quad (6)$$

Numerical analysis is used to obtain seawater mass temperature values at the surface; the approach used is finite volume [25]. The equation used in the software solver to assist with calculations is the Navier-Stokes equation in the first law of thermodynamics, which calculates energy transfer, namely heat, thermodynamic work, and mass transfer [34]. The general equation used in the solver is as follows:

$$\rho\left[\frac{\partial h}{\partial t} + \nabla.(hv)\right] = -\frac{\partial p}{\partial t} + \nabla.(k\nabla T) + \emptyset \quad (7)$$

$$\frac{\partial(E_T)}{\partial t} + (E_t.\nabla) = -p.\nabla u - \frac{1}{Re_d Pr_d}\nabla q\left(\frac{\partial q_x}{\partial x} + \frac{\partial q_y}{\partial y} + \frac{\partial q_z}{\partial z}\right) + \frac{1}{Re_d}u.\nabla\left(u\tau_{xx} + u\tau_{xy} + u\tau_{xz}\right) \quad (8)$$

Where ρ is the density of seawater (kg/m^3); *h* is enthalpy (kJ/kg); *t* is time (s); *p* is pressure (bars); *Et* is total energy (watts); q is heat flux (w/m^2), and u is speed (m/s).

3.2.2. Calculation Steps.

The CWP analysis is carried out into several segments to make numerical calculations easier divided into 9 (ninth) segments (figure 6) [25]. The distance between the pipe in this study is the MGI measurement location and the mainland on Bali Island, namely 5000 m at a depth of 800 m (figure 2), with the assumption that the pipe length using the Pythagorean Theorem is 5064 m.

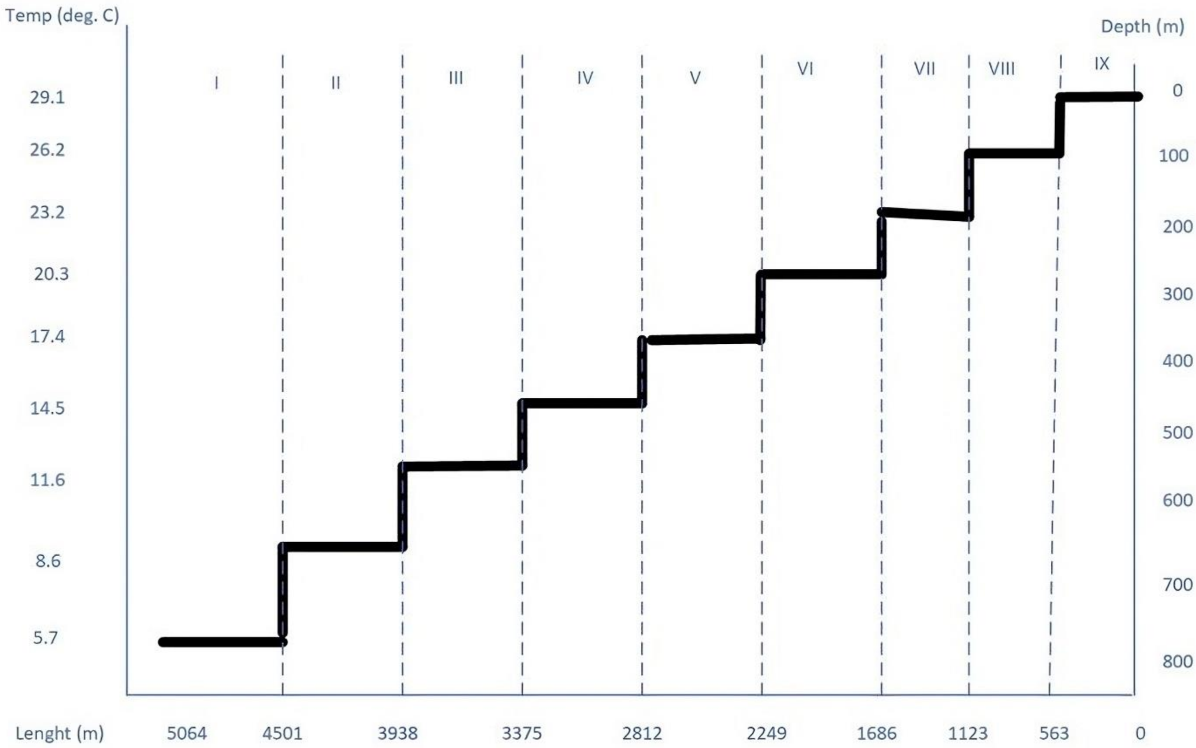

Figure 6. The segmentation of CWP numerical calculation.

4. Results and Discussion

This section employs a fictional OTEC power plant to perform impact factor analyses. The plant's location is characterized by surface seawater temperatures of 29.1 ◦C, seafloor temperatures of 5.1 ◦C, and the seawater depth of approximately 800 meters with a CWP length of 5064 m from the land. Warm seawater from a depth of 0 meters and cold seawater from a depth of 800 meters are pumped with a mass flow of 44.85 kg/s by OTEC. The necessary parameters for material CWP are enumerated in Table 2. Calculations using equations (2)-(6) the heat flux at the CWP surface for each material are presented in table 3.

Table 3. Heat and mass transfer in CWP.

Depth (m)	P_r	R_e	N_u	h_{API5L} W/m².K	$h_{Aluminium}$ W/m².K	h_{HDPE} W/m².K	q_{API5L} W/m²	$q_{Aluminium}$ W/m²	q_{HDPE} W/m²
0	10.7	219,298	877.8	985.3	1415.2	24.2	-2921.7	-4157.0	-70.7
100	10.6	206,844	835.0	952.6	1348.6	24.2	-2832.0	-3955.3	-70.6
200	9.6	194649.5	772.6	904.5	1254.3	24.2	-2679.9	-3654.3	-70.5
300	8.9	182672.6	717.2	858.9	1168.3	24.2	-2526.6	-3358.5	-70.5
400	8.2	170951.7	662.8	811.8	1082.7	24.1	-2343.6	-3024.6	-70.4
500	7.3	159483.9	607.2	761.2	994.6	24.1	-2093.2	-2607.9	-70.2
600	6.9	147906.2	560.6	716.4	919.4	24.0	-1743.7	-2084.7	-66.6
700	6.4	137061.1	516.6	672.1	847.7	24.0	-1140.7	-1296.9	-68.1
800	5.9	126563.3	473.9	627.4	777.9	23.9	0.0	0.0	0.0

Heat transfer in the mass flow of seawater in the CWP is influenced by seawater temperature based on depth and pipe material because Heat is always transferred from hot objects to cold objects [33]. Based on table 3, the value of $q_{HDPE} < q_{API5L} < q_{aluminium}$, namely the amount of Heat released to the seawater mass in the CWP for aluminium material, is greater than for the other two materials. This phenomenon can be attributed to the higher heat flux exhibited by aluminium, resulting in enhanced heat transfer [35][36]. The heat flux value indicates that the heat transfer process is significantly affected by the choice of CWP material utilized.

The application of numerical analysis utilizing the finite volume method on the CWP is conducted by partitioning it into nine distinct segments, as depicted in figure 6. The obtained results indicate that the utilization of HDPE material for the CWP exhibits comparatively lesser fluctuations in the temperature of the surrounding seawater when compared to the other two materials, as illustrated in figure 7. That is because the thermal conductivity of k_{HDPE} is lower than that of k_{API5L} and $k_{aluminum}$, resulting in reduced heat transfer within the HDPE material [35][37].

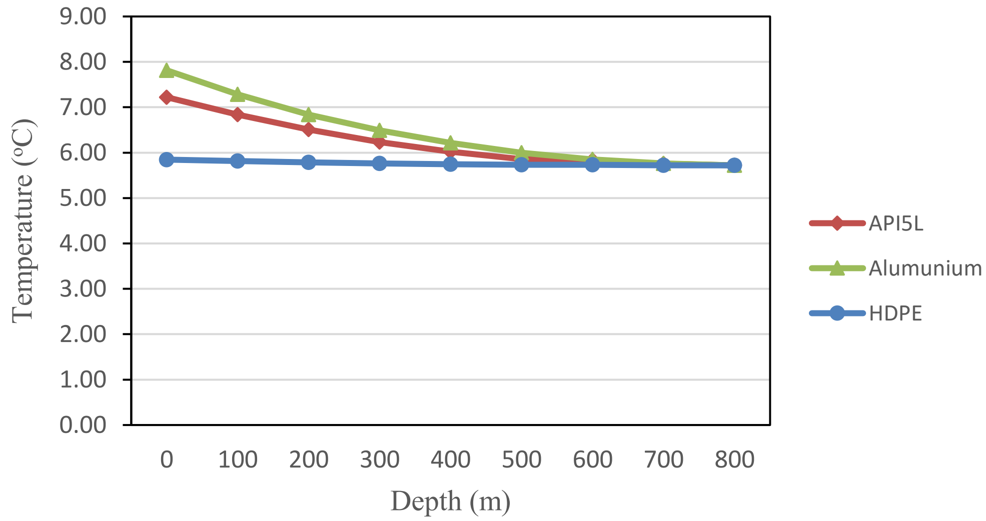

Figure 7. Temperature distribution of the cold seawater in CWP with materials of HDPE, aluminium, and API 5 L.

The numerical calculations performed in this study were verified using equations (2)-(6). These equations were utilized to determine the temperature of the CWP from API 5L and aluminium materials at a specific depth range of 800-700 m along 563 m. The sea water temperature was recorded as 8.6 ºC. The resulting temperatures for the CWP were found to be 5.76 ºC and 5.76 ºC, corresponding to different seawater temperatures. The results align with the outcomes of the conducted numerical calculations (figure 8), indicating that numerical analysis can ascertain seawater temperature in the CWP.

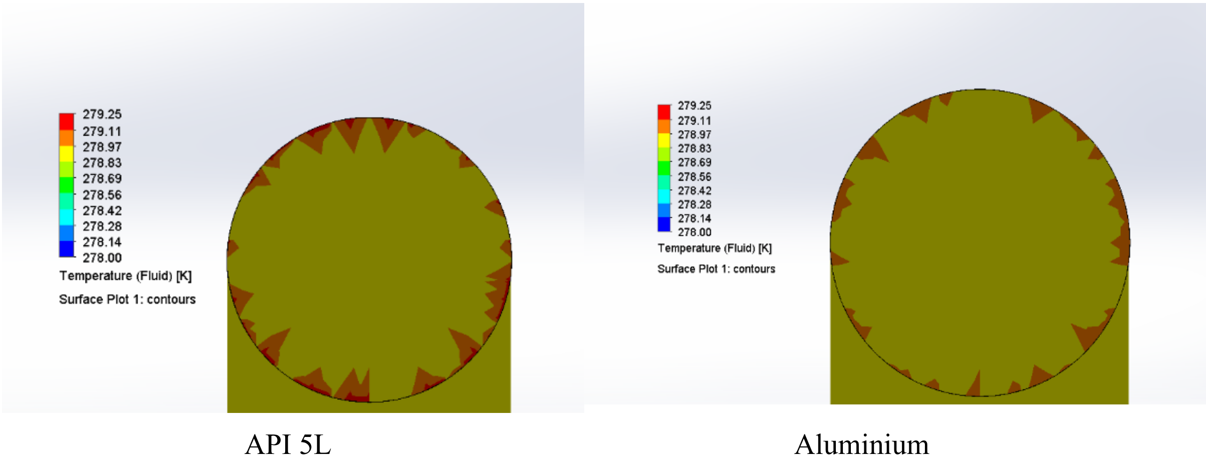

Figure 8. Radial distribution of outlet temperature with materials of API 5L and Aluminium.

5. Conclusion

The results of this study provide preliminary information that the design of OTEC systems with long CWP must consider the distribution of deep-sea water temperature flowing through the CWP to the surface, as changes in seawater temperature in the CWP occur 1-3^{O}C, which is the accumulation of each change in sea water depth. The selection of appropriate materials should also be considered to produce a more realistic design.

6. References

[1] PT.PLN (persero) 2021 *The National Electricity Supply Master Plan 2021-2030* (Jakarta: PT. PLN (Persero))
[2] President of Republic Indonesia 2022 *Presidential Regulation Number 112 of 2022*
[3] Firmansyah A I, Supriatna N K dan Pranoto B 2023 Design of Ocean Current Blade Turbine 100 kW using Hydrodynamics Simulation Approach *J. Adv. Res. Fluid Mech. Therm. Sci.* **101** 174–85
[4] Yahya N Y, Silvianita S dan Satrio D 2023 A Review of Technology Development and Numerical Model Equation for Ocean Current Energy *IOP Conference Series: Earth and Environmental Science* (Surabaya: IOP Publishing Ltd)
[5] Junianto S, Fadilah W N, Adila A F, Tuswan T, Satrio D dan Musabikha S 2022 State of the Art in Floating Tidal Current Power Plant Using Multi-Vertical-Axis-Turbines *IES 2022* (Surabaya: IEEE)
[6] Madi M, Mukhtasor, Satrio D, Tuswan, Ismail A, Rafi R, Yunesti P, Buana S W dan Jarwinda 2024 Experimental Study on the Effect of Foil Guide Vane on the Performance of a Straight-Blade Vertical Axis Ocean Current Turbine *Nase More* **71**
[7] Satrio D, Suntoyo, Widyawan H B, Ramadhani M A dan Muharja M 2024 Effects of the distance ratio of circular flow disturbance on vertical-axis turbine performance: An experimental and numerical study *Sustain. Energy Technol. Assessments* **63** 103635

[8] Mubarok M A, Arini N R dan Satrio D 2023 Optimization of Horizontal Axis Tidal Turbines Farming Configuration Using Particle Swarm Optimization (PSO) Algorithm *2023 International Electronics Symposium (IES)* vol 1 (Surabaya: IEEE) hal 19–25
[9] Sasmita A F, Arini N R dan Satrio D 2023 Numerical Analysis of Vertical Axis Tidal Turbine: A Comparison of Darrieus and Gorlov Type *2023 International Electronics Symposium (IES)* (Surabaya: IEEE) hal 26–31
[10] Aulia A, Athallah A G, Albasyir M A, Selvia S P, Darisman H A dan Satrio D 2023 Study of Diameter-to-Draft Ratio of Pitch Point Absorber as Wave Energy Converter in Indonesia Waters Based on Boundary Element Method *IOP Conference Series: Earth and Environmental Science* (Surabaya: IOP Publishing Ltd)
[11] Lestari S, Mukhtasor M, Satrio D dan Rahmawati S 2023 Oceanographic survey on current due to breaking wave for energy generations : a case study of Pacitan bay , East Java , Indonesia *IOP Conference Series: Earth and Environmental Science* (Surabaya: IOP Publishing Ltd)
[12] Fakhri M H, Satrio D dan Suntoyo 2023 Numerical analysis of drag coefficient for damping plate on the submerged body of two-body point absorber device as wave energy converter *International Conference on Green Energy, Computing and Intelligent Technology (GEn-CITy 2023)* (IEEE Xplorer)
[13] Trenggono M, Hidayat R R, Cahyo T N, Mahardiono M D dan Destrianty A D 2021 An assessment Indonesia's Ocean Thermal Energy Conversion (OTEC) as an electrical energy resource *IOP Conference Series: Earth and Environmental Science* vol 746
[14] Martin G. Brown 2021 *White Paper Ocean Thermal Energy Conversion Otec* (Aberdeen)
[15] Ariansyah M N, Diana L dan Satrio D 2022 Numerical Study the Effect of Gap Ratio on Flow Characteristics and Heat Transfer in Staggered Tube Banks *IOP Conference Series: Earth and Environmental Science* vol 972 (Surabaya: IOP Publishing Ltd) hal 012065
[16] Simangunsong R G, Amalia R dan Satrio D 2021 Numerical Analysis of a Shell and Tube Heat Exchanger Using Computational Fluid Dynamics Software *International Electronics Symposium 2021: Wireless Technologies and Intelligent Systems for Better Human Lives, IES 2021 - Proceedings* (Surabaya: IEEE) hal 630–5
[17] Kurniawati I, Pratilastiarso J dan Satrio D 2020 Analysis of the Effect of Cooling Water Condenser to Power Plant Cycle Using Cycle-Tempo Software *IES 2020 - International Electronics Symposium: The Role of Autonomous and Intelligent Systems for Human Life and Comfort* (Surabaya: IEEE) hal 37–42
[18] Jung J-Y, Lee H S, Kim H-J, Yoo Y, Choi W-Y dan Kwak H-Y 2016 Thermoeconomic analysis of an ocean thermal energy conversion plant *Renew. Energy* **86** 1086–94
[19] Upshaw C R 2012 *Thermodynamic and Economic Feasibility Analysis of a 20 MW Ocean Thermal Energy Conversion (OTEC) Power* (The University of Texas at Austin)
[20] Lennard D O N E 1978 Ocean thermal energy. *Altern. Energy Sources, an Int. Compend.* **4**, **Indire** 511–20
[21] Adiputra R dan Utsunomiya T 2019 Stability based approach to design cold-water pipe (CWP) for ocean thermal energy conversion (OTEC) *Appl. Ocean Res.* **92** 101921
[22] Habib M I, Adiputra R, Prabowo A R, Erwandi E, Muhayat N, Yasunaga T, Ehlers S dan Braun M 2023 Internal flow effects in OTEC cold water pipe: Finite element modelling in frequency and time domain approaches *Ocean Eng.* **288**
[23] Komang N, Andayani S, Ilahude D dan Satriadi A 2020 Studi Potensi OTEC Berdasarkan Distribusi Suhu , Salinitas dan Densitas di Perairan Timur – Utara Pulau Bali *Indones. J. Oceanogr.* **02** 10–1
[24] Ilahude D, Yuningsih A, Permanawati Y, Yosi M, Zuraida R dan Annisa N 2020 Site Determination for OTEC Turbine Installation of 100 MW Capacity in North Bali Waters Penentuan Lokasi Turbin OTEC dengan Kapasitas 100 MW di Perairan Bali Utara *Bull. Mar. Geol.* **35** 1–12

[25] Mao L, Wei C, Zeng S dan Cai M 2023 Heat transfer mechanism of cold-water pipe in ocean thermal energy conversion system *Energy* **269**
[26] Gallup D L, Smith P C, Star J F dan Hamilton S 2005 West Seno Deepwater Development Case History–Production Chemistry *SPE International Symposium on Oilfield Chemistry* (The Woodlands, Texas: SPE)
[27] Lidyana V 2021 Butuh Rp 300 M Benahi 3 Anjungan Offshore yang Nganggur *detikfinance* 2–6
[28] Umah A 2021 Heboh 100 Anjungan Migas RI ' Nganggur ', Ternyata Ini Sebabnya *CNBC Indones.* 3–8
[29] Ridwan M 2021 Pembongkaran Anjungan Migas, Skema Cost Recovery Bisa Jadi Opsi *Bisnis Indones.* 1–5
[30] Vega L A 2010 Economies of ocean thermal energy conversion (OTEC): An update *Proceedings of the Annual Offshore Technology Conference* vol 4 hal 3239–56
[31] Vega L A 1992 Economics of Ocean Thermal Energy Conversion (OTEC) *Ocean Energy Recover.* 152–81
[32] American Petroleum Institute 2018 Line Pipe API Specification 5L 205
[33] Incropera F P, DeWitt D P, Bergman T L dan Lavine A S 2007 *Fundamentals of Heat and Mass Transfer*
[34] PANAHI-KALUS H, AHMADINEJAD M dan MOOSAIE A 2020 The effect of temperature-dependent viscosity and thermal conductivity on velocity and temperature field: an analytical solution using the perturbation technique. *Arch. Mech.* **72** 555–76
[35] Ausloos M 2001 Thermal Conductivity *Encycl. Mater. Sci. Technol.* 9151–5
[36] Shashi Menon E 2015 *Fluid Flow in Pipes*
[37] GRIMVALL G 1999 Thermal Conductivity *Thermophys. Prop. Mater.* 255–85

Acknowledgments
The authors are grateful to the Institut Teknologi Sepuluh Nopember (ITS), for fully funding this study through the grant contract numbers: 2414/PKS/ITS/2023 and 1950/PKS/ITS/2023. The authors also appreciate to Dwi Purnomo Hendradhata for supporting the study.